Published in final edited form as:
Lab Chip. 2008 December ; 8(12): 2105–2112. doi:10.1039/b810329a.

Photolithographic patterning of organosilane monolayer for generating large area two-dimensional B lymphocyte arrays†

Nan Li and **Chih-Ming Ho**
Center for Cell Control and Department of Mechanical and Aerospace Engineering, Henry Samueli School of Engineering and Applied Science, University of California, Los Angeles, CA, 90095, USA. E-mail: chihming@seas.ucla.edu

Abstract

High-density live cell array serves as a valuable tool for the development of high-throughput immunophenotyping systems and cell-based biosensors. In this paper, we have, for the first time, demonstrated a simple fabrication process to form the hexamethyldisilazane (HMDS) and poly (ethylene glycol) (PEG) binary molecular surface which can be used to effectively form high fidelity cell arrays. The HMDS self-assembled monolayer (SAM) on glass substrates was photolithographically patterned and its ability to physically adsorb proteins was characterized by contact angle measurement and fluorescence microscopy respectively. Passivation of the non-HMDS coated background by PEG was verified to have no impact on the pre-patterned HMDS and greatly inhibited the non-specific protein binding. Using the biotin–streptavidin complexation as an intermediate, uniform orientation and high bioactivity were achieved for the immobilized B lymphocyte specific anti-CD19 antibodies and therefore ensured the formation of high resolution B lymphocyte arrays. The cell–ligand interaction specificity was investigated and the anti-CD19 decorated micropatterns presented a much higher cell-capturing rate (88%) than those modified by non-specific ligands (15% for anti-CD5 and 7% for streptavidin). The approach was verified to be biocompatible and the properties of the antibody-modified surface were maintained after 12 h cell culture. The HMDS monolayer formation and patterning processes, and the universal HMDS/biotin-BSA/streptavidin template, provide a very simple and convenient process to generate high resolution micropatterns of cell-adhesive ligands and are extendable to form arrays of other types of cells as well.

Introduction

The inception of micro-electro-mechanical systems (MEMS) in the late 1980s has enabled the miniaturization of transducers at the length scale commensurate with biological cells.[1] The integration of microfluidic actuators, such as microvalves, micro-pumps, and micromixers, with on-chip biosensors has greatly improved the efficiency and sensitivity of biological assays.[2,3] Current lab-on-a-chip technologies, with increased system level integration, have become the heart of point-of-care devices allowing for rapid detection, high diagnostic efficiency, and low reagent consumption.[4] One attractive application is to use live cells as the biosensing elements in that their cellular machinery and signaling pathways can be exploited *in vitro* to enhance the specificity and sensitivity of the detection scheme.[5] The phenomenal successes of microtransducer manufacturing in the past decades have shifted the research emphasis of lab-on-a-chip systems from device fabrication to the engineering of surface molecular properties. The focus now lies in improving the detection limit of biotransducers,

†Part of a special issue on Point-of-care Microfluidic Diagnostics; Guest Editors—Professor Kricka and Professor Sia.

Correspondence to: Chih-Ming Ho.

which is essentially determined by the amount of non-specific molecular binding and strongly depends on the surface property of the device. For point-of-care diagnostics, live cell-based biosensors can be exploited to detect the presence of certain analytes in body fluids and screen for toxic reagents.[6,7] Spatially controlling the organization of large quantities of cells into precisely defined regions, ideally at the single-cell scale, is also dependent on the modification of surface molecular properties.[8–11] The invention of new biofunctional materials and advancements in surface molecular patterning are therefore always of great interest for point-of-care applications.

Self-assembled monolayer (SAM), a well-ordered monomolecular layer formed spontaneously by the reaction of certain types of molecules with supporting solid materials, has been widely explored to modulate the surface properties in order to enhance or prevent cell attachment.[12–14] Arrays of SAMs can be defined by a variety of micro- and nano- patterning methods such as microcontact printing,[15] photolithography,[16] scanning probe lithography,[17] electron-beam lithography,[18] and ink-jet printing.[19] These micro- and nano- patterns of SAMs can be subsequently coupled with extracellular matrix (ECM) proteins or peptides, antibodies, and other biomolecules to control the selective attachment of both anchorage-dependent and non-adherent cells to the substrates. Two typical families of SAMs are alkanethiol reacting with gold and organosilane reacting with oxidized surfaces.[14] Compared to alkanethiol SAM formation which needs a special gold deposition procedure, organosilane SAMs can be directly formed on transparent substrates such as glass and quartz, which is especially applicable for biological studies to achieve high resolution imaging.[20] Another essential requirement for high selective cell patterning is to render the areas beyond the desired cell-adhesion regions inert to resist bio-fouling. Among several non-fouling molecular systems, poly-(ethylene glycol) (PEG) has attracted increased interest in its effectiveness for preventing non-specific protein binding.[13,21–23] The highly hydrated PEG chains can minimize the interaction of proteins with the substrate and thus suppress bio-fouling. The combination of SAM micropatterning and PEG passivation provides a powerful research tool for a variety of applications such as genomics, proteomics, drug discovery, and molecule or cell-based biosensing.

In this paper, we demonstrated a molecular engineered system combining organosilane and PEG for the successful generation of large area two-dimensional B lymphocyte arrays. Hexamethyldisilazane (HMDS), a commonly used photoresist adhesion promoter in micromachining, was self-assembled on the glass substrate by vapor phase deposition and was patterned by photolithography. The patterned HMDS served as a template to anchor antibodies for immunocapturing the B cells. The background was passivated with PEG through the silanization reaction of PEG–silane and hydroxyl group terminated glass surface in order to prohibit the non-specific protein binding. The PEG passivation process was verified to have no impact on pre-fabricated HMDS micropatterns and the effectiveness of PEG in preventing bio-fouling ensured the high cell patterning selectivity. The hydrophobic characteristics of the HMDS monolayer can directly anchor proteins onto the substrate through hydrophobic–hydrophobic interactions with no need for complex chemical reactions. To achieve uniform orientation and high bioactivity for the immobilized antibodies, a biotin–streptavidin complexation guided immobilization scheme was explored instead of directly immobilizing antibodies onto the patterned HMDS template. Such a patterning scheme not only retained the biofunctionality of immobilized proteins as shown in our previous study,[23] but also demonstrated the ability to generate B lymphocyte arrays with effective patterning areas up to the centimeter scale in this paper. The generated antibody patterns retained the cytophilic properties and the viability of B lymphocytes was investigated to be well-maintained after 12 h culture on the antibody micro-patterns. The simplicity and generality of this patterning method can be applied to other types of non-adherent or weak-adherent cells such as leukocytes, stem cells, and cancer cells, and therefore it extends the patterning capability of the current techniques which were mostly focused on adherent cell patterning.[24] In addition,

photolithography ensures the creation of arrays of HMDS micropatterns with high spatial resolution and the precise alignment of these micropatterns relative to any reference elements on the chip. Such characteristics make this cell patterning technique especially suitable for integrating live cells into lab-on-a-chip systems to detect toxins and biomolecules for point-of-care applications.[7]

Experimental

Materials

HMDS was purchased from Shin-Etsu Microsi Inc. (Phoenix, AZ). AZ5214-E photoresist and AZ400K developer were purchased from Hoechst Celanese (Somerville, NJ). 2-[Methoxy (polyethyleneoxy)propyl]trimethoxysilane (PEG–silane, M_w = 460–590) was purchased from Gelest, Inc. (Morrisville, PA). Glass slides (75 mm × 25 mm), 35 mm diameter sterile Petri dish, hemocytometer, tissue culture flasks, phosphate buffered saline (1× PBS, pH = 7.2), and Mediatech cellgro RPMI-1640 modified culture medium (with 2 mM L-glutamine and 25 mM HEPES) were purchased from Fisher Scientific (Pittsburgh, PA). Phenol red-free RPMI-1640 modified culture medium, triethylamine, formaldehyde, acetone, isopropyl alcohol (IPA), anhydrous toluene, and ethanol were purchased from Sigma-Aldrich Chemical Co. (St. Louis, MO). Bovine serum albumin (BSA), biotin conjugated BSA (biotin–BSA), Texas Red conjugated streptavidin (TR–streptavidin), and Immunopure® streptavidin were purchased from Pierce Biotechnology, Inc. (Rockford, IL). Fetal bovine serum (FBS), penicillin/streptomycin antibiotics, and CellTracker™ green (5-chloromethylfluorescein diacetate, CMFDA) were purchased from Molecular Probe (Eugene, OR). Biotinylated mouse anti-human anti-CD5 and anti-CD19 antibodies were purchased from BD Pharmingen (San Diego, CA). Human Burkitt's lymphoma B cell-line (DG75) was obtained from America Type Culture Collection (Manassas, VA).

HMDS monolayer patterning and PEG passivation

The procedures for patterning HMDS monolayer using photolithography and backfilling the background with PEG–silane on glass substrates were the same as previously reported.[23] Fig. 1(a) illustrates the fabrication process. In brief, each standard 75 mm × 25 mm glass slide was firstly diced into 3 pieces of 25 mm × 25 mm substrates using a dicing machine. After thoroughly cleaning the substrates with Piranha solution (4: 1 of H_2SO_4: H_2O_2) and dehydration baking at 150 °C for 15 min, the substrates were immediately placed into a flask containing saturated HMDS vapor and allowed to slowly cool down for 15 min for vapor phase deposition to form the HMDS monolayer. Positive photoresist AZ5214-E was then spun on the HMDS monolayer and patterned by UV exposure through a chrome photomask. The exposed photoresist as well as the underlying HMDS monolayer were removed by an alkaline AZ400K developer. A two-minute oxygen plasma treatment (500 mTorr, 200 W) was followed to remove the photoresist and HMDS residues. The undeveloped photoresist was dissolved with acetone and rinsed with IPA and deionized (DI) water (18.3 MΩ cm) to reveal the underlying HMDS micropatterns. For PEG passivation, HMDS derivatized glass substrates were placed into 3 mM of PEG–silane dissolved in anhydrous toluene with 1% (v/v) triethylamine as a catalyst for 4 h. To remove the physically adsorbed PEG–silane moieties, the substrates were then sonicated in anhydrous toluene, ethanol and DI water for 5 min respectively and dried with nitrogen. The surface characteristics of the HMDS and PEG monolayers were quantified by water contact angle measurement using a goniometer (First Ten Ångstroms, Portsmouth, VA). The HMDS/PEG–silane modified substrates were either used immediately for cell patterning experiments or stored inside a desiccator until used. The molecular structures of HMDS and PEG after reacting with hydroxyl (–OH) group terminated glass substrate are shown in Fig. 1(b).

Antibodies immobilization

For antibodies immobilization, 0.5 mL of biotin–BSA (50 μg/mL) was first pipetted onto the HMDS/PEG–silane modified glass substrate and incubated at 4 °C for 30 min. Then 0.5 mL of Immunopure® streptavidin (or TR–streptavidin for fluorescence imaging) (20 μg/mL) was incubated at room temperature for 10 min and followed by incubation of 0.5 mL of biotinylated mouse anti-human anti-CD19 (or anti-CD5 as controls) monoclonal antibodies (10 μg/mL) at room temperature for 15 min. After each incubation, the substrate was rinsed with 1× PBS three times to remove any unbound proteins and gently dried with nitrogen.

Cell culture and fluorescence staining

DG75 B lymphocytes were cultured in RPMI-1640 culture media supplemented with 2 mM L-glutamine, 10% FBS, 100 U mL^{-1} penicillin, and 100 mg mL^{-1} streptomycin in a 5% CO_2/95% air humidified incubator at 37 °C. For generation of B lymphocyte arrays, DG 75 cells were collected and centrifuged at 500 *g* for 5 min at 4 °C and resuspended in 1× PBS. The cell concentration was determined using a hemocytometer. The cell viability was assessed by Trypan blue exclusion both before and after cell patterning. The dead cells turn to a dark color after Trypan blue staining. The prepared cells were used within 1 h for the patterning experiments.

For fluorescence imaging, cells were stained with CellTracker™ green following the manufacturer instructions. In detail, cells were first harvested by centrifugation at 500 *g* for 5 min at 4 °C and then the supernatant was aspirated. The cells were resuspended in phenol red-free RPMI-1640 culture media to avoid auto-fluorescence with 5 μM CellTracker™ green supplemented. Cells were kept cultured in a 5% CO_2/95% air humidified incubator at 37 °C for 30 min. Then the aforementioned cell preparation procedure was followed for the cell patterning experiments.

Formation of B lymphocyte arrays

25mm × 25mm glass substrates with immobilized mouse anti-human anti-CD19 (or anti-CD5 as controls) antibodies were placed into a 35 mm diameter sterile Petri dish. 0.5 mL of the prepared cell suspension was gently added to cover the whole substrate and allowed to seed for 30 min at room temperature. Upon completion of patterning, the substrates were transferred into another 35 mm diameter sterile Petri dish containing 5 mL of 1× PBS with 3.7% formaldehyde (v/v) and incubated for 15 min at room temperature to fix the cells. Finally, the sample was turned over and gently dipped into fresh 1× PBS three times to remove the unbound cells.

Imaging the protein and cell patterns

The formed patterns of TR–streptavidin and B lymphocytes (stained by CellTracker™ green) were observed through the rhodamine (535 ± 50 nm/610 ± 75 nm) and fluorescein (480 ± 40 nm/535 ± 50 nm) excitation/emission filters of a Leica DMIRB inverted fluorescence microscope, respectively. An equipped monochrome CCD camera (Roper Scientific Photometrics, CoolSnap HQ) with a pixel size of 6.45 μm × 6.45 μm was used for capturing the images.

Results and discussion

Scheme for immunocapturing B lymphocytes

Proteins have been shown to interact predominantly with a hydrophobic surface through hydrophobic–hydrophobic interactions.[25] Therefore the hydrophobic methyl ($–CH_3$) termination of HMDS monolayer is favorable for protein adsorption and can serve as a template

to guide the selective protein immobilization. However, when proteins have been immobilized onto a solid surface, they display heterogeneous binding characteristics, including the target binding affinity and association/dissociation kinetics, from the state in solution. This behavior can be attributed to the limited available receptor binding sites due to the protein immobilization. The variable orientations of immobilized proteins, the steric hindrance, the impact of chemical microenvironments near the solid surface, and the conformation change or even the denaturation of the immobilized proteins are possible reasons for the reduced target binding behavior.[26] Studies showed that the heterogeneity of the immobilized proteins can be reduced by selecting proper protein immobilization strategies through surface chemical reactions or bio-specific interactions.[24,26,27] In our study, the streptavidin–biotin complex was selected as a supporting matrix. Besides the high binding affinity and specificity of the streptavidin–biotin complex, the multiple biotin binding sites of the streptavidin allow for further coupling of the biotinylated antibodies to immunocapture cells. Previous studies showed that the best antibody homogeneity can be achieved through the biotin/streptavidin/biotin–antibody scheme with similar antigen–antibody binding behaviors as those in solution.[26] Our previous results also demonstrated that this immobilization scheme retained the protein biofunctionality very well through studies of the antigen–antibody specific recognition and the enzyme catalysis activity.[23] Biotin–BSA was first physisorbed onto HMDS micropatterns. The free biotin molecules can subsequently anchor the intermediate streptavidin layer to achieve uniform orientations and minimized conformation changes. The other un-occupied biotin binding sites on this streptavidin layer were used to further couple the biotinylated antibodies for cell patterning purposes. The schematic representation of the cell immobilization scheme explored in our study is illustrated in Fig. 1(c).

Protein immobilization on HMDS/PEG–silane modified glass substrate

HMDS ($(CH_3)_3$ Si–NH–Si $(CH_3)_3$) reacts with surface hydroxyl groups ($Si_{(substrate)}$–OH) and forms the trimethylsiloxy ($Si_{(substrate)}$–O–Si–$(CH_3)_3$) groups through the silylation reaction.[17,28]

$$2(Si_{(substrate)} - OH) + (CH_3)_3Si - NH - Si(CH_3)_3 \rightarrow 2(Si_{(substrate)} - O - Si - (CH_3)_3) + NH_3$$

The substrate surface was rendered to be hydrophobic due to the methyl termination of the formed HMDS monolayer. This hydrophobic characteristic leads to improved adhesion for the photoresist and it is also the reason that this silylation reaction is commonly used in semiconductor and MEMS manufacturing for photoresist adhesion promotion. The formed $Si_{(substrate)}$–O–Si bond is very robust to resist organic solvents such as acetone and toluene, but it is susceptible to hydrolysis under high pH conditions. Therefore, after the UV exposed positive photoresist has been developed, the alkaline-based photoresist developer can further attack the underlying HMDS monolayer. This is the principle for using photolithography to pattern HMDS monolayer. The hydrolysis procedure recovered the surface hydroxyl groups on the exposed glass surface. These hydroxyl groups can covalently react with PEG–silane through the silanization reaction. On the contrary, PEG–silane has no interactions with the trimethylsiloxy groups. Therefore PEG molecules should only stay on the non-HMDS covered glass substrate and can effectively passivate the background against protein adsorption.

The degree of the surface hydrophobicity in relation to the HMDS vapor priming time was quantified by water contact angle measurement and the result is shown in Fig. 2(a). Three samples were analyzed at each time point. The pristine glass substrate was hydrophilic with a water contact angle less than 10°. The surface presented to be more hydrophobic after HMDS priming and the hydrophobicity kept increasing as the HMDS priming time increased. After

15 min priming, the maximum of 75 ± 2° water contact angle was achieved. The water contact angle of PEG–silane modified glass surface was measured to be 34 ± 1°. These results are comparable with previously reported values for HMDS and PEG monolayer.[22,29,30] In order to evaluate the effects of the PEG passivation procedure on HMDS monolayer, the glass substrate fully covered with HMDS monolayer was incubated in the PEG passivation solution for 24 h. The water contact angle was measured after the sample has been thoroughly rinsed and dried. No distinct contact angle change was observed compared to the original HMDS monolayer derivatized surface. This result indicated that PEG passivation process has no impact on the existing HMDS monolayer.

The protein adsorption ability of HMDS monolayer was investigated using BSA as a model protein. The water contact angle was measured to decrease to 55 ± 2° after incubating BSA on the HMDS monolayer for 10 min, which indirectly indicated the successful adsorption of BSA onto the HMDS surface. Studies have shown that physisorbed proteins on hydrophobic surfaces can be desorbed from the surface by detergents.[31,32] Here, a nonionic detergent, polysorbate 20 (Tween 20), was used to desorb the physisorbed BSA from the HMDS surface. The process was monitored by water contact angle measurement. As shown in Fig. 2(b), cyclical Tween 20 washes could repeatedly remove the physisorbed BSA from the HMDS surface. After each wash, the water contact angle was recovered to the same level as the one for pristine HMDS surface, *i.e.* 75 ± 2°. This result verified that BSA was physisorbed onto the HMDS surface through hydrophobic–hydrophobic interactions. However, as controls, the physisorbed BSA on HMDS surface was quite stable in the ionic buffer and the water contact angle was measured to remain almost unchanged after the immersion of the sample inside 1× PBS for 24 h.

The selective protein immobilization capability of HMDS and PEG–silane modified surface was characterized by fluorescence microscopic observation. Fig. 3(a) shows the fluorescence image of TR–streptavidin binding to the physisorbed biotin–BSA on a HMDS/PEG–silane derivatized glass substrate. The proteins stayed exclusively on the HMDS modified grid patterns with an interconnecting line width of 10 μm, a junction circle diameter of 50 μm, and nine squares of 10 μm × 10 μm within each grid. High signal-to-noise ratio was achieved by analyzing the fluorescence intensity profile between the PEG modified areas and the HMDS modified areas which were coated with TR–streptavidin (Fig. 3(b)). The fluorescence signal on the PEG modified areas was at the same level as the background glass substrate, which verified the effectiveness of PEG for suppressing the non-specific protein binding. The well-ordered HMDS and PEG molecular structures and their abilities to mediate protein adsorption resulted in the sharp fluorescence signal contrast between HMDS and PEG–silane modified regions and ensured the high cell patterning resolution. To confirm the specific binding of streptavidin to the biotin molecules, control experiments were performed to incubate TR–streptavidin on HMDS surface treated by BSA instead of biotin–BSA. The fluorescence signal from biotin–BSA treated HMDS sample was quantified and shown to be much higher than those from the BSA treated and pristine HMDS surfaces (Fig. 3(c)). This result verified that the attachment of TR–streptavidin was through the bio-specific interaction between streptavidin and biotin molecules instead of the non-specific adsorption. The high specificity of the biotin–streptavidin coupling resulted in an active and uniformly oriented streptavidin layer, which ensured the further binding of biotinylated antibodies with high efficiency and affinity.

Formation of B lymphocyte arrays

DG75 cells express a generic B lymphocyte surface antigen CD19. The immobilized biotinylated mouse anti-human anti-CD19 antibodies were demonstrated to be able to specifically anchor DG75 cells onto patterned areas with single cell patterning resolution. Fig. 4(a) shows the fluorescence image of an array of B lymphocytes (stained by CellTracker™

green) captured by biotinylated anti-CD19 antibodies which were immobilized through underlying biotin–BSA and streptavidin layers. In this array, the 10 micrometer-sized patterns are compatible with the size of the B cell and therefore most 10 micrometer-sized patterns were occupied by single B lymphocytes. Images taken under higher magnification (Fig. 4(b) and (c)) show more detailed characteristics of the generated B lymphocyte arrays. The 10 μm lines were almost exclusively occupied by single cells. The 10 μm × 10 μm squares also showed single cell anchorage capabilities.

The binding specificity between B lymphocytes and the surface immobilized ligands was assessed by comparing the B lymphocyte adhesion on anti-CD19, anti-CD5 and streptavidin modified micropatterns. Streptavidin only has high binding specificity to biotins. CD5 is a surface antigen expressed on T lymphocytes and anti-CD5 antibody should have no interactions with B lymphocytes. Therefore, both molecules are non-specific to the investigated B lymphocytes. B lymphocytes were incubated either on anti-CD19 and anti-CD5 antibody modified samples through the intermediate streptavidin layer or directly on streptavidin modified samples using the same patterns illustrated in Fig. 3(a). To evaluate the cell capturing ability, patterning areas of 2 mm × 2 mm were randomly selected from each sample modified by anti-CD19, anti-CD5, or streptavidin. In each area, there are 900 of 10 μm × 10 μm squares and only these squares were analyzed. The number of 10 μm × 10 μm squares with cells occupied was manually counted in each area under the microscope. The cell capturing rate was calculated by dividing this number by the total number of 900. As shown in Fig. 5, anti-CD19 antibody presented a much higher cell capturing rate (88%) than that obtained from anti-CD5 antibody and streptavidin modified samples, which was only 15% and 7% respectively. This result clearly showed that the B lymphocyte arrays were mainly generated through the specific interactions between the cell membrane antigens and the immobilized antibodies. It also indicated that the bioactivities of the immobilized anti-CD19 antibodies were well retained to effectively immunocapture the B lymphocytes.

In addition, the relation between the cell concentrations and the resulting cell patterning quality was investigated. The optimal concentration was found to be in the 5×10^6 cells/mL range. Concentrations outside this window generated more defects and resulted in worse patterning quality. For example, higher cell concentration (5×10^7 cells/mL as tested) generated large cell clusters in the patterned areas. These clusters were more prone to be washed together off the substrate and resulted in a large amount of empty spots on the array. However, lower cell concentration (5×10^5 cells/mL as tested) was not sufficient for generation of the high-density cell arrays and the patterns can be barely recognized.

The long term stability of the generated cell-adhesive (anti-CD19 antibody) and cell-resistive (PEG–silane) surface was tested by culturing the patterned B lymphocytes in the RPMI-1640 media supplemented with FBS and antibiotics for up to 12 h. Fig. 6 shows the optical images of patterned B lymphocytes after 12 h culture. The cells were confined only in the areas presenting the anti-CD19 antibodies. Furthermore, the cell viability was assessed using Trypan blue staining before and after culturing. It was visually estimated that more than 94% of the cultured cells were still alive after 12 h culture, which was almost the same as the living cell percentage before culturing (96%). The long term culturing capability and surface stability revealed the non-fouling characteristics of the PEG and the biocompatibility of the employed cell patterning scheme.

However, some imperfections were observed for the generated B lymphocytes arrays, including multiple cells in one adhesion spot and empty spots not occupied by any cells. Such imperfections can be minimized by further optimization of the experimental protocol. For example, it has been shown that biotinylation of the cell membrane proteins in combination of the surface immobilized biotinylated antibody improved the patterning quality in the

streptavidin mediated cell patterning approach.[24] In this way, the increased binding strength between the antibody template and the cells enhances the patterning controllability. Also, combining this patterning method with microfluidic networks in the future would be beneficial. Compared to the manual washing process currently adapted in our method, microfluidics can achieve better patterning quality due to the accurate controllability of the shear stress applied to the immobilized cells. By facilitating the antibody delivery and immobilization with microfluidic networks, it is also possible to pattern multiple cell types, the subsets of leukocytes for instance, on a single chip. This would be especially useful for panning and characterizing multiple leukocyte subsets in parallel and greatly benefit researches such as immunophenotyping and high-throughput image-based leukocyte differetiation.[33,34] Furthermore, understanding the formed HMDS and PEG monolayers at the molecular scale would enable us to better control the surface properties and consequently extend the applications of this surface engineering approach.

Conclusion

In summary, we have developed a novel HMDS/PEG molecular engineered system for generation of large area two-dimensional B lymphocyte arrays on the glass substrate. In combination with the high affinity biotin–streptavidin complexation, this system was able to generate high resolution micropatterns of functional proteins in a stepwise fashion and successfully guide the selective cell attachments. Photolithographically patterned HMDS monolayer was favorable for protein physisorption whereas the backfilled PEG–silane eliminated the non-specific protein adhesion to a great extent so that high cell patterning resolution at single-cell level was realized. Instead of using a “lift-off” process usually involved in a photolithography patterning approach to selectively remove the cell-adhesive proteins, our method avoids the exposure of proteins to harsh chemicals whereas the merits of photolithography patterning, such as creation of high resolution protein microarrays with well-ordered feature size, shape, and pitch, were still achieved. The straightforward chemistry and the simple fabrication technique employed in this method provide a convenient tool for studies involving protein and cell patterning. In addition, the generality of utilizing the streptavidin–biotin interaction to immobilize the antibodies can be easily extended to pattern a large number of cell types simply by altering the choice of biotinylated antibodies.

Acknowledgments

This research has been supported by NASA National Space Biomedical Research Institute (NCC 9-58-317), and partially by NSF nano manufacture center SINAM (DMI-0327077) and NIH nanomedicine program (Center for Cell Control, PN2EY018228). The authors would like to thank Fuqu Yu from Dr Ren Sun’s lab in the Department of Molecular and Medical Pharmacology of UCLA for providing the cells.

References

1. Ho CM, Tai YC. Annu Rev Fluid Mech 1998;30:579–612.
2. Zhang CS, Xing D, Li YY. Biotechnol Adv 2007;25:483–514. [PubMed: 17601695]
3. Marcus JS, Anderson WF, Quake SR. Anal Chem 2006;78:3084–3089. [PubMed: 16642997]
4. Tüdős AJ, Besselink GAJ, Schasfoort RBM. Lab Chip 2001;1:83–95. [PubMed: 15100865]
5. El-Ali J, Sorger PK, Jensen KF. Nature 2006;442:403–411. [PubMed: 16871208]
6. Rothermel A, Kurz R, Ruffer M, Weigel W, Jahnke HG, Sedello AK, Stepan H, Faber R, Schulze-Forster K, Robitzki AA. Cell Physiol Biochem 2005;16:51–58. [PubMed: 16121033]
7. Asphahani F, Zhang M. Analyst 2007;132:835–841. [PubMed: 17710258]
8. Folch A, Toner M. Annu Rev Biomed Eng 2000;2:227–256. [PubMed: 11701512]
9. Park TH, Shuler ML. Biotechnol Progr 2003;19:243–253.

10. Falconnet D, Csucs G, Grandin HM, Textor M. Biomaterials 2006;27:3044–3063. [PubMed: 16458351]
11. Jung DR, Kapur R, Adams T, Giuliano KA, Mrksich M, Craighead HG, Taylor DL. Crit Rev Biotechnol 2001;21:111–154. [PubMed: 11451046]
12. Blawas AS, Reichert WM. Biomaterials 1998;19:595–609. [PubMed: 9663732]
13. Castner DG, Ratner BD. Surf Sci 2002;500:28–60.
14. Chechik V, Crooks RM, Stirling CJM. Adv Mater 2000;12:1161–1171.
15. Mrksich M, Whitesides GM. Trends Biotechnol 1995;13:228–235.
16. Mooney JF, Hunt AJ, McIntosh JR, Liberko CA, Walba DM, Rogers CT. Proc Natl Acad Sci USA 1996;93:12287–12291. [PubMed: 8901573]
17. Sugimura H, Nakagiri N. J Photopolym Sci Technol 1997;10:661–666.
18. Zhang GJ, Tanii T, Zako T, Hosaka T, Miyake T, Kanari Y, Funatsu TW, Ohdomari I. Small 2005;1:833–837. [PubMed: 17193534]
19. Pardo L, Wilson WC, Boland TJ. Langmuir 2003;19:1462–1466.
20. Lussi JW, Tang C, Kuenzi PA, Staufer U, Csucs G, Voros J, Danuser G, Hubbell JA, Textor M. Nanotechnology 2005;16:1781–1786.
21. Franks W, Tosatti S, Heer F, Seif P, Textor M, Hierlemann A. Biosens Bioelectron 2007;22:1426–1433. [PubMed: 17055243]
22. Lan S, Veiseh M, Zhang MQ. Biosens Bioelectron 2005;20:1697–1708. [PubMed: 15681184]
23. Li N, Ho CM. JALA 2008;13:237–242.
24. Kim H, Doh J, Irvine DJ, Cohen RE, Hammond PT. Biomacromolecules 2004;5:822–827. [PubMed: 15132667]
25. Ostuni E, Grzybowski BA, Mrksich M, Roberts CS, Whitesides GM. Langmuir 2003;19:1861–1872.
26. Vijayendran RA, Leckband DE. Anal Chem 2001;73:471–480. [PubMed: 11217749]
27. Neubert H, Jacoby ES, Bansal SS, Iles RK, Cowan DA, Kicman AT. Anal Chem 2002;74:3677–3683. [PubMed: 12175153]
28. Sugimura H, Nakagiri N. Langmuir 1995;11:3623–3625.
29. Hirotsu T. J Appl Polym Sci 1979;24:1957–1964.
30. Luo JT, Wu WF, Wen HC, Wan BZ, Chang YM, Chou CP, Chen JM, Chen WN. Thin Solid Films 2007;515:7275–7280.
31. Sigal GB, Mrksich M, Whitesides GM. J Am Chem Soc 1998;120:3464–3473.
32. Deval J, Umali TA, Lan EH, Dunn B, Ho CM. J Micromech Microeng 2004;14:91–95.
33. Revzin A, Sekine K, Sin A, Tompkins RG, Toner M. Lab Chip 2005;5:30–37. [PubMed: 15616737]
34. Sekine K, Revzin A, Tompkins RG, Toner M. J Immunol Methods 2006;313:96–109. [PubMed: 16822521]

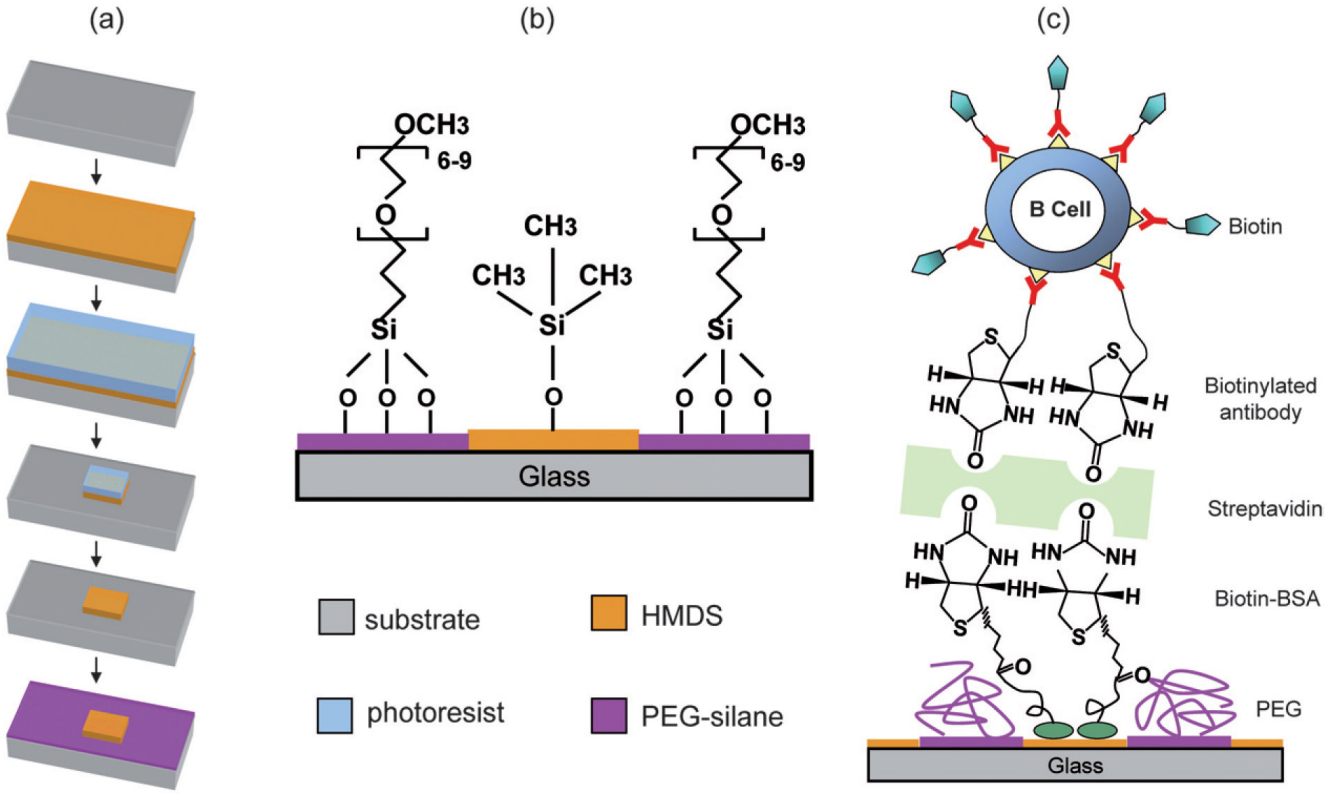

Fig. 1.

Process for generating two-dimensional B lymphocyte arrays. (a) Fabrication procedure for creating the protein immobilization template. HMDS monolayer was coupled onto hydroxyl-group terminated glass substrates through silylation reactions and patterned by photolithography. The non-HMDS covered areas were passivated with PEG–silane to prevent the non-specific protein binding. (b) Schematic representation of molecular structures of PEG and HMDS after reacting with the surface hydroxyl groups. (c) Illustration of protein immobilization scheme for generating large area two-dimensional B lymphocyte arrays.

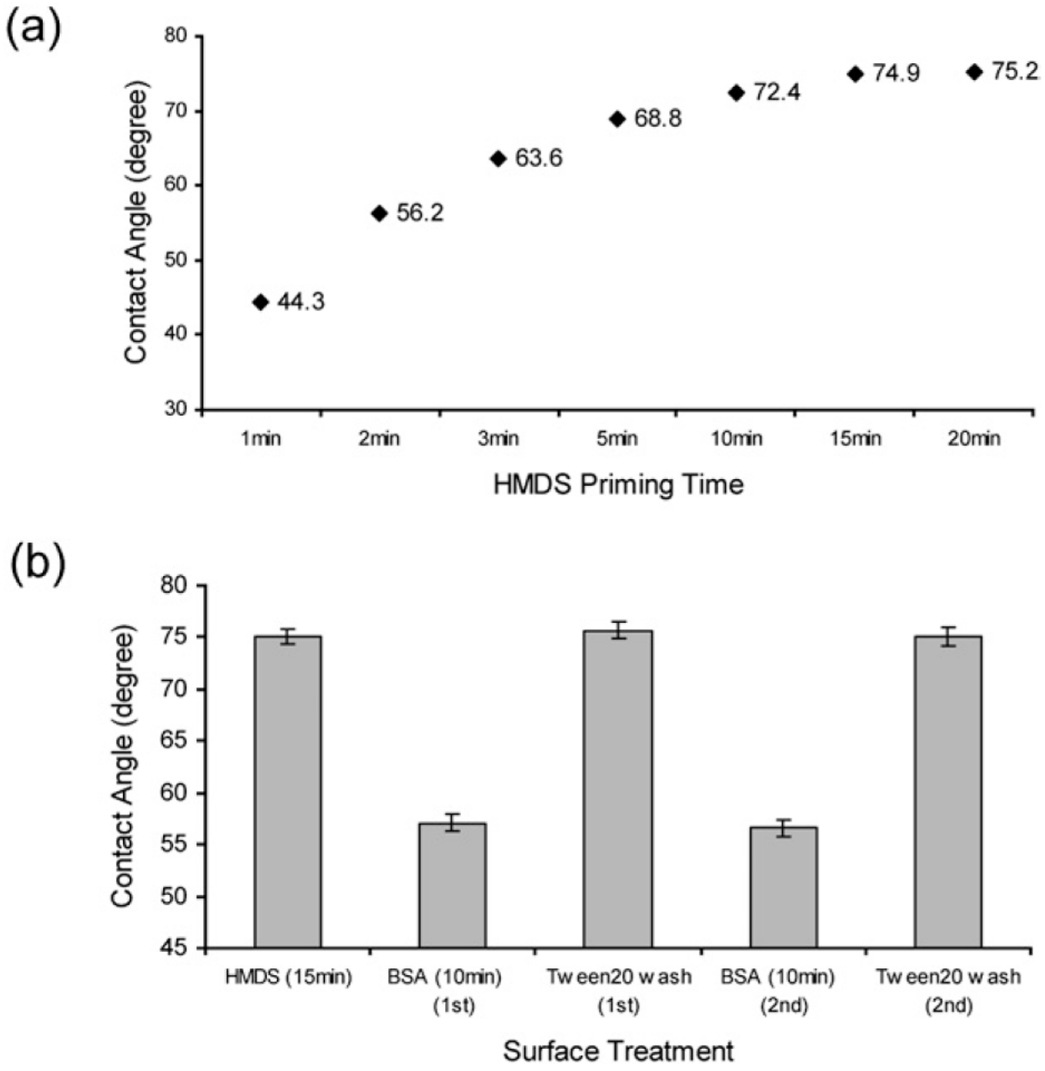

Fig. 2.

Characterization of the HMDS monolayer surface properties and protein physisorption process with water contact angle measurement. (a) The measured water contact angles in relation to HMDS vapor priming time. (b) Measurement of water contact angles as results from cyclical BSA adsorption on HMDS surface and Tween 20 washes.

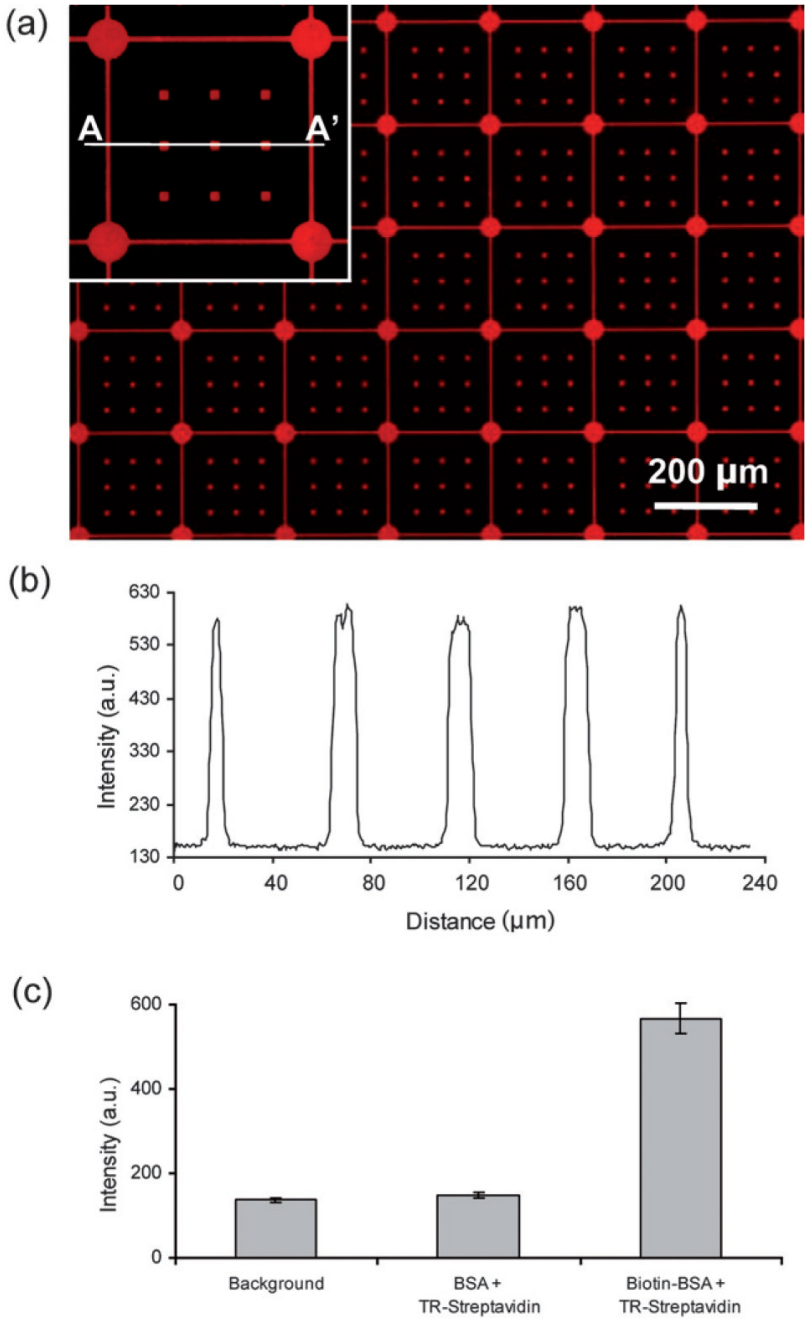

Fig. 3.

(a) Fluorescence micrograph of the TR–streptavidin interacting with the physisorbed biotin–BSA on the HMDS/PEG–silane modified glass substrate. (b) Fluorescence intensity profile of A–A′ cross section in (a). (c) Fluorescence intensity of TR–streptavidin after incubation on the BSA and biotin–BSA coated HMDS surfaces in comparison with the HMDS background.

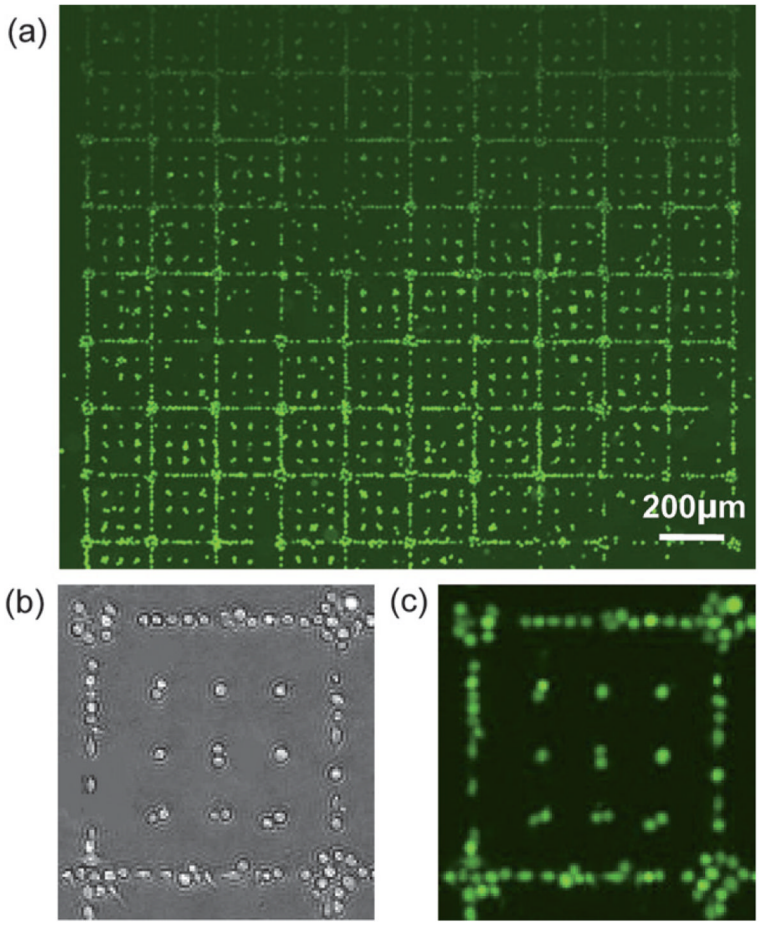

Fig. 4.

Generated large area two-dimensional B lymphocyte arrays. (a) Fluorescence micrograph of the generated B lymphocyte (stained by CellTracker™ green) arrays using biotin–streptavidin complexation guided immobilization of mouse anti-human anti-CD19 antibodies. Optical (b) and fluorescence (c) micrographs of one grid area reveal the single cell patterning capability.

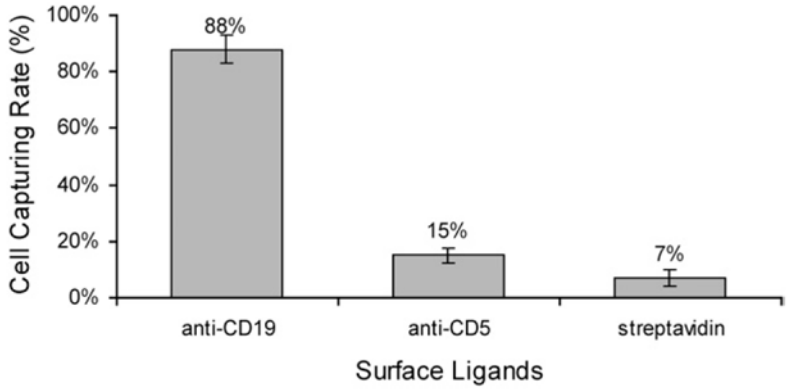

Fig. 5.

Specificity of the B lymphocyte interaction with anti-CD19, anti-CD5, and streptavidin modified micropatterns. B lymphocyte specific ligands, anti-CD19, showed a much higher cell capturing rate compared to the non-specific anti-CD5 and streptavidin.

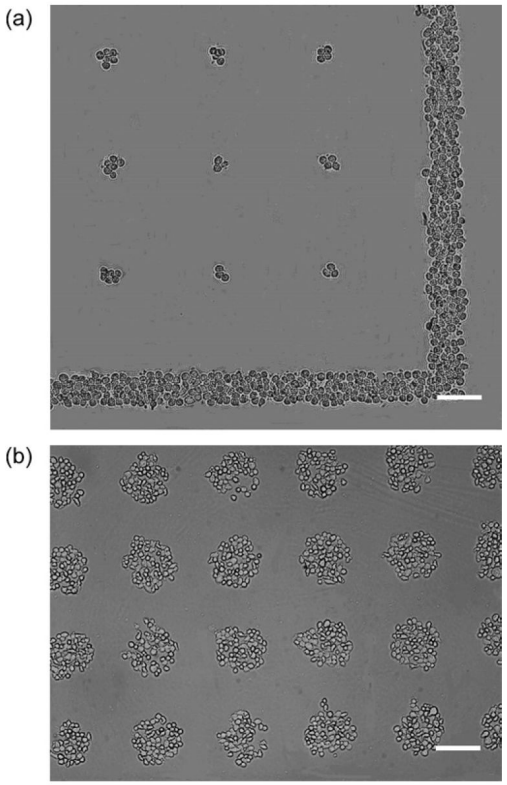

Fig. 6.
Optical micrographs of the patterned B lymphocytes after 12 h culture. Cells only stayed at the areas where the mouse anti-human anti-CD19 antibodies were presented. Scale bar: 100 μm.